TABLE I. Neck frequencies and belly/neck ratios as measured, and derived belly frequencies for copper, silver, and gold.

Material	F_N (G)	F_B/F_N	F_B (G)
Cu[a]	$(2.174\pm0.002)\times10^7$	26.72 ± 0.02	$(5.809\pm0.006)\times10^8$
Ag	$(8.921\pm0.01)\times10^6$	51.56 ± 0.05	$(4.600\pm0.005)\times10^8$
Au	$(1.532\pm0.001)\times10^7$	29.33 ± 0.03	$(4.493\pm0.004)\times10^8$

[a] Similar figures for copper, supplied to Dr. E. Zornberg, resulted in an improved fit to a 1-electron-per-atom model (Ref. 7). However, it is not necessarily suggested that the figures in JT (Ref. 3) are *all* in error by +0.6%, as Zornberg assumed.

errors due to hysteresis in a superconducting solenoid will be rather small where a relatively large field interval is involved. This is not generally the case in a direct measurement of a belly frequency. We have found, indeed, that a value of F_B obtained by sweeping the field over an interval of some 1% may be 1 or 2% high in comparison with that derived from $F_N(F_B/F_N)$. However, if a 10% interval is used this error is reduced to less than +0.3%. It is even possible in this way to calibrate the error for a particular 10% or so field interval for use in measuring a de Haas–van Alphen frequency in which no transfer via a ratio can be made.

Note added in proof. Since submitting this paper we have become aware of the work published by O'Sullivan and Schirber.[12] Of the noble metals they give figures for copper only: these figures agree with ours to within our combined experimental errors of ±0.2%.

[12] W. J. O'Sullivan and J. W. Schirber, Cryogenics **7**, 118 (1967).

PHYSICAL REVIEW VOLUME 161, NUMBER 3 15 SEPTEMBER 1967

Annealing Studies of Irradiated Platinum*

M. J. ATTARDO AND J. M. GALLIGAN†
Brookhaven National Laboratory, Upton, New York
(Received 31 March 1967)

A field-ion microscope operated at 4.2°K has been used to study defects introduced into 99.9998% pure platinum by fast-neutron irradiation. Damaged or depleted zones have been identified and their concentration and size have been studied as a function of dose and annealing temperature. Direct observations indicate a distribution of zone sizes up to approximately 40 Å in diameter. The density of these zones is linear with dose in the range from 10^{16}–10^{18} n/cm^2 ($E>1.45$ MeV). Field-ion-microscope studies also reveal that upon annealing through stage-IV recovery, the small depleted zones (<15 Å) grow, causing an increase in the density of zones in the range between 15–30 Å. Simultaneously, the largest of the depleted zones present collapse to form dislocation loops lying on {110} planes. The remaining depleted zones are removed at temperatures corresponding to that of self-diffusion. Stage-III recovery in platinum has also been studied by examining specimens irradiated at temperatures above and below stage-III recovery. Direct observation indicates that some form of interstitial-atom motion must be associated with this recovery stage. The possibility of vacancies moving in this temperature range is specifically ruled out by energy considerations.

I. INTRODUCTION

IRRADIATION of metals with energetic particles can introduce local displacements of atoms, leading to nonequilibrium concentrations of Frenkel defects and various combinations of vacancies and of interstitials.[1] At very low temperatures, it is expected that such defects would be immobile except for close pair annihilation of Frenkel defects, which are separated by less than a minimum distance.[2] Various annealing studies of irradiated materials above such low temperatures have revealed five distinct stages of recovery in many of the fcc and bcc metals investigated.[3] Further correlation of these recovery stages with such material parameters as individual melting points of the materials involved, indicate that similar processes might be taking place in corresponding temperature ranges, using the melting point as the scaling factor.[4] This is most likely a consequence of the fact that the energetics of the process do not involve the fine detail of the specific lattice. However, the detailed interpretation of the observed spectrum, within the general framework of imperfection theory, has not been agreed upon by

* This work was performed under the auspices of the U. S. Atomic Energy Commission.
† Present address: Columbia University, New York, New York.
[1] An extensive review of the theoretical aspects of this problem has been given by D. K. Holmes, in *The Interaction of Radiation with Solids*, edited by R. Strumane, J. Nihoul, R. Gevers, and S. Amelinckx (North-Holland Publishing Company, Amsterdam, 1964).
[2] T. R. Waite, Phys. Rev. **107**, 463 (1957); **107**, 471 (1957).
[3] H. G. Van Bueren, *Defects in Solids* (North-Holland Publishing Company, Amsterdam, 1960); A. C. Damask and G. J. Dienes, *Point Defects in Metals* (Gordon and Breach Science Publishers, New York, 1963), p. 60.
[4] J. Moteff and J. P. Smith, American Society for Testing Materials Report No. 380, p. 171, 1964 (unpublished).

many active in the field.[5–8] This lack of agreement has generally involved the interpretation of the defect or defects involved in stage-III recovery. Two distinct schools of thought have arisen which employ the following interpretations.

The first school, as represented by Corbett, Smith, and Walker, considers stage III to be associated with the removal of interstitials from impurity traps, and the simultaneous migration of vacancies in stage III. The other viewpoint as given by Meechan, Sosin, and Brinkman[9] and Seeger[10] considers stage III to be associated with the removal of dumbbell interstitials and that single vacancies are removed in stage IV. They consider no trapping of interstitials to be involved in the process. Two recent publications have summarized the opposing viewpoints[11,12] so that no more details need be given here, except to say that we consider neither school's arguments definitive on the question.

The above arguments apply to isolated single defects which are formed in individual encounters with energetic particles—simple displacements—or defects that are products of some form of focusing[13] away from very drastic changes in the local lattice disturbance.[14–16] Such local disturbances of the lattice are of interest for a variety of reasons, but mainly because they are considered to be responsible for many of the mechanical property changes of irradiated crystals.[16] The size and detailed shape of these local disturbances as well as their distribution, has been inferred from transmission electron microscopy, in some instances after annealing in stage III has occurred. It should be mentioned, though, that it is not possible to distinguish between vacancy and interstitial agglomerates, except under very favorable circumstances.[17] In the particular case of neutron-irradiated platinum, Ruedl *et al.*[18] have not been able to discern any damage by standard transmission electron microscopy techniques.

We have previously reported on some studies of the defects introduced into platinum by fast-neutron irradiation,[19] which have since been extended to higher integrated fluxes. Stages III and IV recovery in this material occur in the temperature ranges of 223 to 323°K and 473 to 673°K, respectively.[20] The results of this, as well as some studies of the effect of annealing upon the measured depleted zone distribution, are given below.

II. EXPERIMENTAL PROCEDURE

A. Material

The platinum used in this experiment was special-lot platinum, obtained from Englehardt Industries, Inc., with a reported purity level of 99.9998%. The manufacturer states further that this material has the highest measured thermal emf to date. The thermal emf is considered to be a reliable measure of purity in platinum, more so than resistivity ratio.[21] A spectrographic analysis was undertaken of this material and no impurities were detected.

Prior to irradiation of the material, the 0.002-in. diam wire was annealed at 1300°C which produced a (100) or (111) wire texture. This in itself indicates that grain boundaries have moved through the bulk of the material and thereby lowered the dislocation density and possibly reduced some of the impurities in the bulk through preferential adsorption of impurities by sweeping boundaries.

B. Microscopic Observation and Characterization of the Material

The major tool used in this study was a field-ion microscope, operated at 4.2°K, for the examination of platinum specimens. This microscope, which has been previously described,[22] is fully bakeable and after a mild bakeout (200°C) pressures of the order of 10^{-9} are attained. After this initial bakeout no additional baking was required. This is important in establishing that contamination is in no way a contributor to the experiments at hand. With this background pressure, no serious contamination of a specimen would occur in approximately 10^3 sec without a field present. A schematic diagram, Fig. 1, shows the pumping system, the ancillary equipment used in the operation of the microscope, and a schematic of the microscope itself. Prior to undertaking the main experiments on studies of radiation damage, a large number (30) of well-annealed, high-purity platinum specimens were examined to ascertain what image quality could be expected in

[5] J. W. Corbett, R. B. Smith, and R. Walker, Phys. Rev. **114**, 1452 (1959); **114**, 1460 (1959).
[6] A. K. Seeger, Phys. Letters **8**, 296 (1964).
[7] G. D. Magnuson, W. Palmer, and J. S. Koehler, Phys. Rev. **109**, 1990 (1958).
[8] W. Bauer and A. Sosin, Phys. Rev. **147**, 482 (1966).
[9] C. Meechan, A. Sosin, and J. Brinkman, Phys. Rev. **120**, 411 (1960).
[10] A. Seeger, P. Schiller, and H. Kronmüller, Phil. Mag. **5**, 853 (1960).
[11] R. von Jan, Phys. Status Solidi **17**, 361 (1966).
[12] J. W. Corbett, *Electron Radiation Damage in Semi-Conductors and Metals*, edited by F. Sietz and D. Turnbull (Academic Press Inc., New York, 1966), p. 200.
[13] R. M. Silsbee, J. Appl. Phys. **28**, 1246 (1957).
[14] J. A. Brinkman, J. Appl. Phys. **25**, 961 (1954).
[15] F. Seitz and J. S. Koehler, *Solid State Physics*, edited by F. Seitz and D. Turnbull (Academic Press Inc., New York, 1956), Vol. II p. 307.
[16] A. K. Seeger, in *Proceedings of the Second International Conference on the Peaceful Uses of Atomic Energy* (United Nations, Geneva, 1958), Vol. VI, p. 250.
[17] W. Bell, D. Maher, and G. Thomas, in *Lattice Defects in Quenched Metals*, edited by R. Cotterhill, M. Doyama, J. J. Jackson, and M. Meshii (Academic Press Inc., New York, 1965).
[18] F. Reudl, P. Delavignette, and S. Amelinckx, *Radiation Damage in Solids*. I (International Atomic Energy Agency, Vienna, 1962), p. 363.
[19] M. J. Attardo and J. M. Galligan, Phys. Rev. Letters **7**, 191 (1966).
[20] W. Bauer and A. Sosin, Phys. Rev. **147**, 482 (1966).
[21] H. Zysk (private communication).
[22] M. J. Attardo, J. M. Galligan, and J. Sadofsky, J. Sci. Instr. **43**, 607 (1966).

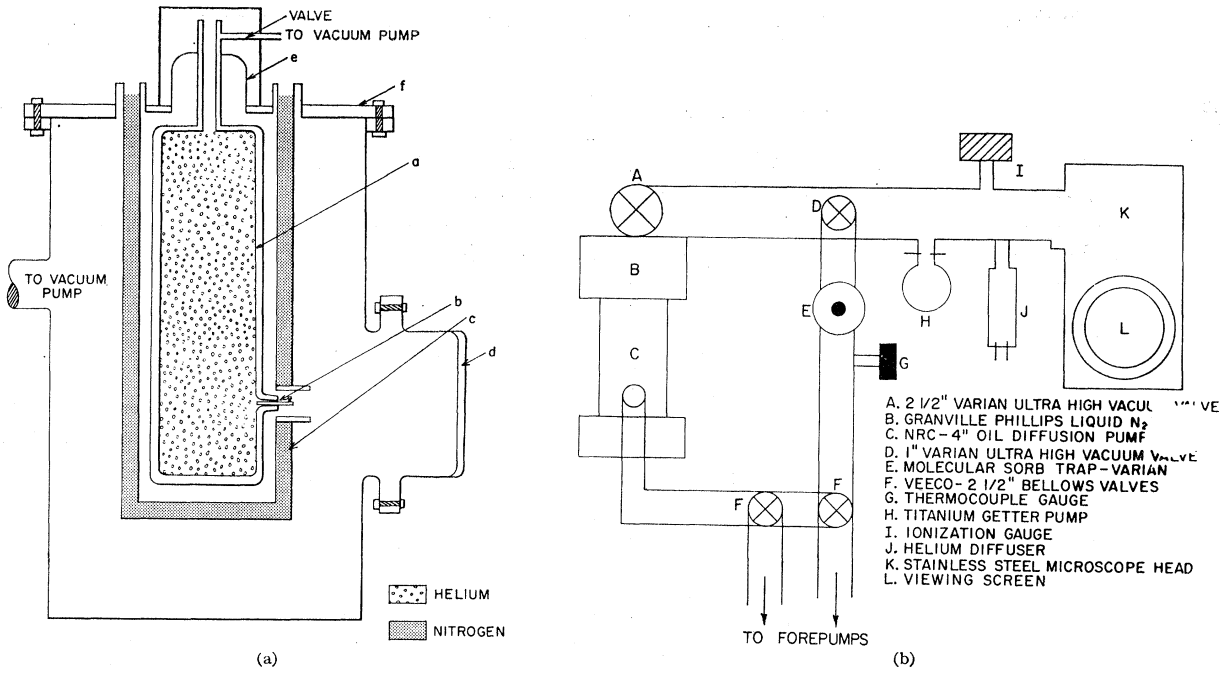

FIG. 1. Schematic diagram of low-temperature field-ion microscope and ancillary equipment.

operation at 4.2°K and to establish the standard state of the material.

In this study some effects were observed in particular crystallographic areas of the specimen,[23] which were peculiar to these areas only. We believe that these defects, which are peculiar to the [102] plane, are due to the electrostrictive effect of the field, which is highest on the [102] planes. The regularity of the surface, other than in this region, was extremely reproducible from specimen to specimen. This as well as direct correlation with different integrated fluxes used in the present experiment, to be discussed below, is a good indication that the field ion microscope is a powerful tool for studies of defect structures in certain metals as has been pointed out before.[23] These blank experiments also allowed an assessment of the maximum concentration of subsurface interstitials present in the as-received material. Since we record more than 60 photographs per imaged specimen which has developed a final end form, we can assess the maximum concentration of interstitials as follows:

The number of atoms observed in the blank experiments was of the order of 30 tips$\times$60 planes$\times 10^4$ atoms in normal lattice sites $=1.8\times10^7$ atoms. In these observations no displaced atoms were observed. Thus, the upper limit for the interstitial atom fraction was $1/10^7$. The tip-making procedure was similar to that recommended by Müller[24] and fracture of tips, while imaging, occurred in about 50% of the specimens examined. If a specimen fractured during observation, no subsequent data were recorded on that specimen and all previous data recorded on that specimen were discarded. After specimens were initially made and cooled to low temperatures, they were not allowed to be thermally cycled to room temperature until the completion of an individual experiment. This avoided any possibility of strain release which has also been discussed by Müller.[23]

C. Irradiation of Materials

The platinum, after annealing, was irradiated to four integrated fluxes—10^{16}, 10^{17}, 10^{18}, and 5×10^{19} *nvt* ($E>1.45$ MeV). In the case of the platinum irradiated to an integrated flux of 10^{18}, two separate irradiations were performed with the specimens held at two temperatures 100 and 340°K. The 10^{16}, 10^{17}, and 10^{18} irradiations were performed in the Brookhaven National Laboratory Graphite Reactor, while the 5×10^{19} irradiation was performed in the Brookhaven High Flux Beam Reactor.

D. Annealing Procedure

The irradiated material, after appropriate examination in the as-irradiated condition, was annealed at a variety of temperatures. In the material irradiated at 100°K, annealing was performed at 373°K—above stage III[8]—while in the material irradiated at 340°K, annealing was performed at 523, 772, and 873°K. These latter temperatures correspond to slightly below stage IV, above stage IV, and above stage V, respectively.[8]

[23] G. Speicher, W. I. Pimbly, M. Attardo, J. Galligan, and S. Brenner, Phys. Letters **23**, 194 (1966).
[24] E. W. Müller, Advan. Electron. Electron Phys. **13**, 84 (1960).

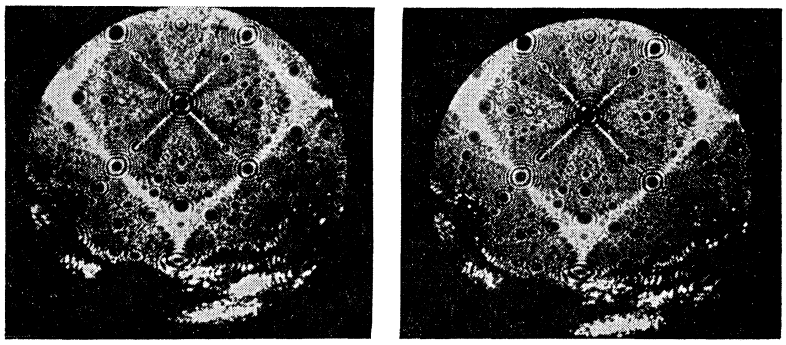

(a) (b)

FIG. 2. Micrograph of platinum specimen bombarded at 4.2°K. Figure 2(a) shows specimen prior to bombardment, while 2(b) shows some interstitial atoms below the surface, as revealed by field evaporation.

All specimens were annealed in a tubular furnace under a flowing argon atmosphere. Control experiments were run in the furnace at 873°K and examination of such specimens, using field ion microscopy, revealed no contamination.

III. EXPERIMENTAL RESULTS

A. Calibration Experiment

It is of interest to first consider a control experiment which bears directly upon the presence of interstitial atoms in irradiated platinum. In this experiment an annealed platinum tip was prepared and imaged at 4.2°K, and then the tip was bombarded with copper particles, in a manner similar to that described by Müller.[25] A large amount of surface damage was thereby introduced. Subsequently, field evaporation was undertaken and some bright spots were observed removed from the surface-damage regions (Fig. 2). Those bright spots are considered to correspond to interstitial atoms for the following reasons:

(a) They are only correlated with damage at a surface; (b) such bright spots persist throughout the field evaporation of more than one layer and, therefore, do not correspond to leftover atoms; (c) when the bright spots are observed in conjunction with condition (a), they are "reached" through field evaporation.

This experiment as well as some annealing studies in the temperature range 4 to 80°K will be reported in more detail in a separate publication.

B. Defects Present Prior to and After Stage-III Annealing

After confirming that the field-ion microscope is capable of revealing the presence of interstitial atoms, we proceeded to study the defect distribution in stage III. Two primary measurements were made of the material before and after annealing it at a temperature above stage III. The atom fraction of interstitial atoms, Fig. 3 (bright spots), was measured as well as the size distribution of depleted zones [Fig. 4(a)]. The concentration of interstitial atoms present prior to annealing above stage III was of the order of 10^{-4} atom fraction. Such bright spots were noticeably anisotropic in shape in that they extended along a line in about 40% of the observed cases. In the remaining 60% of the cases, the bright spots appear as single circularly symmetric spots. A systematic analysis of the direction associated with the major axis of this increased intensity revealed the direction of this axis to be ⟨100⟩. Some arguments about the frequency of occurrence of lines versus spots will be given in the discussion. In addition, the observed concentration of bright spots increased in the vicinity of depleted zones.

Annealing of the irradiated material at 100°C for 10 min was next undertaken and subsequent field-ion-microscope observation revealed that the number of single bright spots and those along a single line were reduced to a very low level, $<10^{-6}$ atom fraction. Secondly, what appears to be clustering of interstitials has now occurred (Fig. 5). In this annealing process the size distribution—within the limits of measurement—has not drastically changed [Fig. 4(b)].

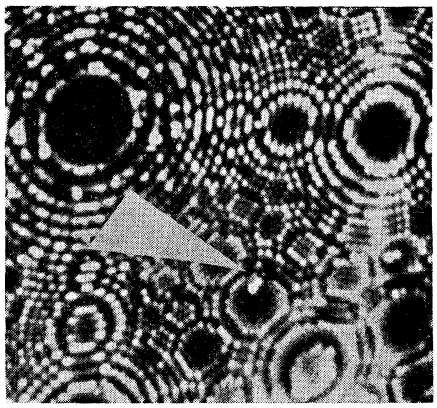

FIG. 3. Bright spots in neutron irradiated platinum, which are present prior to annealing above stage III.

[25] E. W. Müller, *Direct Observation of Imperfections in Crystals* (John Wiley & Sons, Inc., New York, 1962), p. 77.

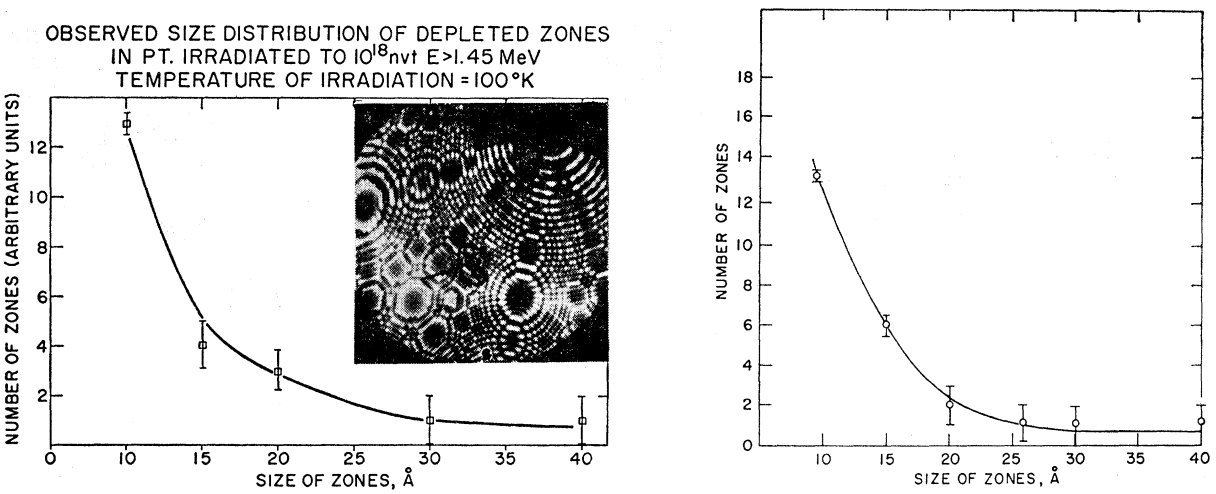

FIG. 4. (a) Size distribution of depleted zones. Photomicrograph of depleted zone in neutron irradiated platinum along with the specimen irradiated at 100°K with fast neutrons ($E>1.45$ MeV) and annealed at 280°K. (b) Size distribution of depleted zones after annealing through stage III.

C. Dose Dependence of Depleted Zones

A composite representation of the dose dependence of the number of depleted zones is given in Fig. 6. In this limited range of integrated flux, the number of depleted zones increases linearly with exposure to fast neutrons.

D. Defects Present Prior to and After Stage-IV Annealing

Specimens were annealed in a temperature range prior to stage-IV recovery, but considerably above stage-III recovery; the results of this are shown in Fig. 7. Also shown in this figure is the depleted zone size distribution versus concentration of zones in the irradiated material, after annealing *above stage IV*. One can surmise from the observed change in the distribution that large vacancy clusters are growing at the expense of small ones. A further observation which substantiates this, and explains why clusters larger than 45 Å in diameter are not seen, is shown in Fig. 8. This is a vacancy dislocation loop, with the plane of the loop lying in a {110}-type plane. The plane of the loop is determined from a field evaporation experiment in which successive removal of layers allows us to map out the plane of the loop in three dimensions. This plane is then compared with a standard stereographic projection and the plane determined. The accompanying sketch shows how we interpret this observed contrast effect as a dislocation loop.

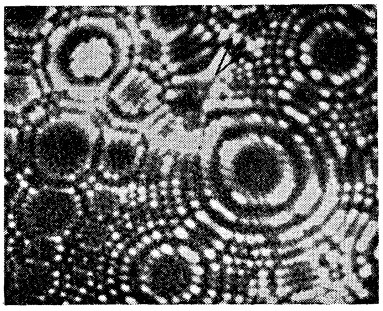

FIG. 5. An example of some defect structures in neutron irradiated platinum after annealing at 373°K.

E. Defects Present After Annealing Irradiated Material Above Stage V

After annealing the material for one hour at 873°K, the observed field-ion microscope patterns were the same as those observed prior to irradiation, from which we conclude that this is the temperature range where the remaining depleted zones have been removed.

IV. DISCUSSION

A. Interstitial Removal in Stage-III Recovery

The low temperature, *in situ* bombardment of platinum quite clearly shows that interstitial atoms can be revealed with the field ion microscope, as has been previously demonstrated in the case of interstitial atoms in tungsten by Sinha and Müller.[26] Such a calibration experiment, accordingly, serves as a check on the presence or absence of interstitials, as well as the form of the interstitials present in irradiated materials, after other recovery stages. Further, indirect arguments are possible, which quite clearly eliminate any possibility that the observed removal of bright spots after annealing through stage III are due to anything except single interstitials. These arguments will now be discussed in turn.

[26] M. K. Sinha and E. W. Müller, J. Appl. Phys. **35**, 1256 (1964).

(i) Impurities. Aside from the fact that the bright spots are directly introduced by irradiation, the observed ratio of interstitials to impurities is 50/1 for this material.

(ii) The density of bright spots in the vicinity of the observed depleted zones is considerably higher than that far removed from a depleted zone.

(iii) Transmuted platinum atoms. In the case of platinum the major transmutation product is gold which, for an integrated flux of 10^{18} fast neutrons, would be present in a concentration of 10^{-6} atom fraction. Furthermore, annealing at 100°C should in no way alter the presence of such gold atoms.

(iv) Vacancies are known to give rise to contrast effects in the field-ion microscope of the opposite sense observed here.[24]

(v) The observed anisotropy of shape of the bright spots in the neutron irradiated material—lines of about two atom diameters and single bright spots—can plausibly be explained as the presence of a split interstitial aligned along ⟨100⟩ direction, as observed. The anistropy depends, of course, upon which way the interstitial configuration is oriented with respect to the surface.

(vi) Annealing above stage III drastically lowers the observed concentration of bright spots.

(vii) The observed size of the bright spots, as well as their anisotropy of shape indicates that they are not di-interstitials.

(viii) Field evaporation through more than one atomic layer at the surface of a neutron irradiated specimen, without the removal of bright spots, shows that the contrast is associated with an arrangement of atoms in a subsurface interstitial position.

(ix) Even if we assume 90% annihilation of interstitial atoms prior to stage III,[27] the observed atom fraction of interstitial atoms is still less than that predicted from the integrated flux used.[28]

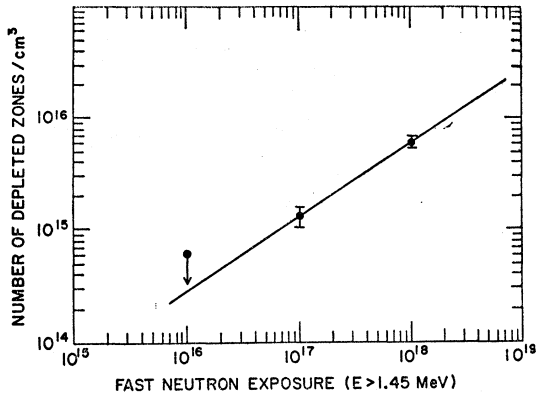

FIG. 6. Integrated flux dependence of the total number of depleted zones in neutron irradiated platinum ($E>1.45$ MeV).

It is of interest to discuss in more detail, some of the arguments which are concerned with trapping of split interstitial atoms by impurity atoms below stage III. Briefly, some interaction—electronic or elastic—is assumed between a displaced atom and an impurity. This is further assumed to be quite large, since the split interstitial is only postulated to be quite mobile at temperatures corresponding to stage III for various materials. These deep traps require that a fraction of the impurity atoms be effective in retaining many interstitials. Assume for the moment that the deeper traps (those effective up to temperatures corresponding to stage III) represent $\frac{1}{2}$ of the impurities. If then 90% of the interstitials have been removed prior to stage III, an estimated atom fraction retained would be 10^{-4}. This, in conjunction with $\frac{1}{2}\times 2/10^{6}$ impurities, would require 100 interstitial atoms around each impurity atom. We observe about 10^{-4} atom fraction of interstitials, but certainly not clusters of 100 interstitials.

Furthermore, the model of interstitial atoms being trapped by an impurity atom requires, for most effective

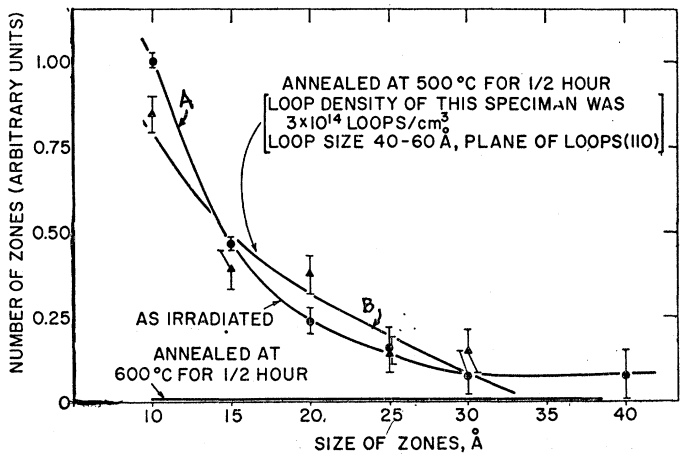

FIG. 7. Changes in size distribution of depleted zones in neutron-irradiated platinum. Curve A shows size distribution of depleted zones after annealing at 373°K and curve B shows the depleted zone size distribution after annealing at 823°K.

[27] R. R. Coltman, Jr., C. E. Klabunde, D. L. McDonald, and J. K. Redman, J. Appl. Phys. 33, 3509 (1962).
[28] L. T. Chadderton, in *Radiation Damage in Crystals* (Methuen Company, Ltd., London, 1965).

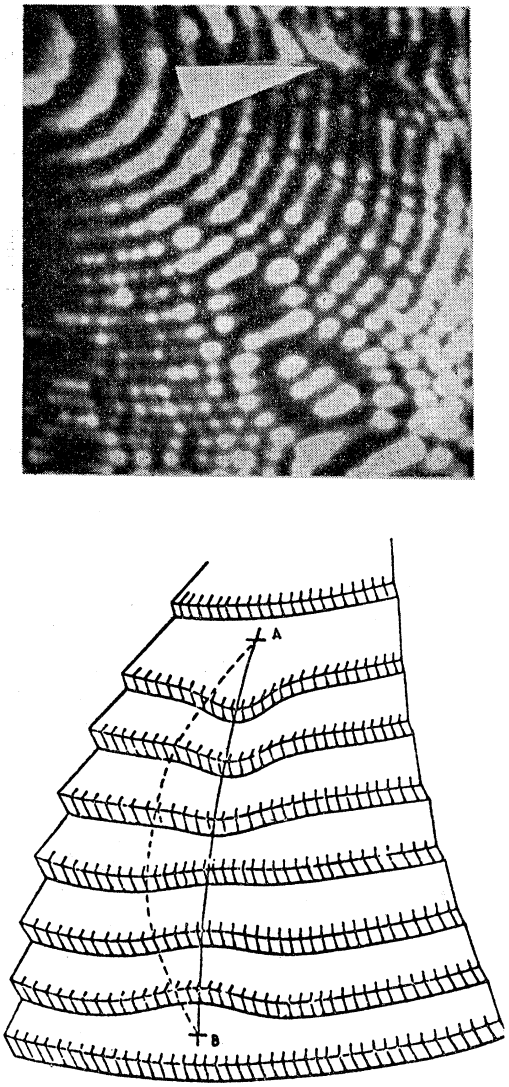

FIG. 8. Vacancy dislocation loop in irradiated platinum after annealing above stage IV (823°K) along with a schematic diagram of contrast effect associated with dislocation loop of approximately 30 Å in size. [After Fortes and Ralph, Phil. Mag. 14, 198 (1966).]

trapping, that the impurity be a "soft" atom since this would form a more effective elastic dipole with an interstitial atom. This, incidentally, implies that the symmetry of such a defect in a solid, is lower than tetragonal as postulated in the internal friction measurements of Seeger and Wagner.[29] Whether or not all impurities in platinum are sufficiently "soft" to bind an interstitial atom is quite questionable; however, there are apparently not enough to account for the observed concentration of interstitial atoms.

Since depleted zones are observed in neutron-irradiated platinum (see Sec. IV B) some focusing of interstitial atoms must occur, which would require both replacement collisions and interstitial crowdion configurations. This indicates that a dynamic crowdion is metastable in platinum, to the extent necessary to give depleted zones.

Another interesting observation which merits some discussion is the "brightening" observed when an interstitial atom approaches a surface layer, Fig. 9. The integrated intensity associated with this configuration is a measure of the protrusion of the surface atoms as a result of a subsurface interstitial. If one naively assumes that the displacements of surface atoms due to an interstitial below the surface are monotonically decreasing with distance, one can arbitrarily fit the experimental curve by assigning displacements of the surface atom of the order of 5% for a separation of two atomic layers, 1% for three atomic layers separation, 0.1% for four atomic layers, and zero for five atomic layers. The expected magnification is calculated in a manner similar to that given by Rose for the case of a small protuberance on a large hemispherical surface. Following Rose,[30] one finds, approximately, for a small protuberance on a hemispherical surface, that a local change in radius changes the local ion current by a maximum of 27 times.[31] This shows up as a magnification factor—an increased intensity over a layer projected area—which only goes to zero when the interstitial is more than four layers away from the surface. It seems unreasonable to expect that impurities or leftover atoms could account for such a result, and in addition, that they would have the *pathological* character that they disappear after annealing at 100°C.

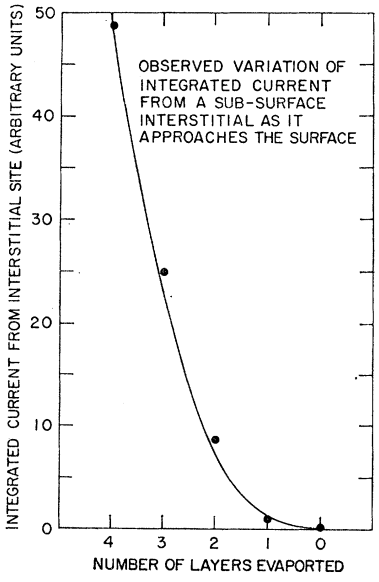

FIG. 9. The integrated intensity associated with a subsurface interstitial at various positions below the surface layers and above.

[29] A. K. Seeger and F. Wagner, Phys. Status Solidi 9, 583 (1965).

[30] D. J. Rose, J. Appl. Phys. 27, 215 (1956).

[31] R. Gomer, *Field Emission and Field Ionization* (Harvard University Press, Cambridge, Massachusetts, 1961).

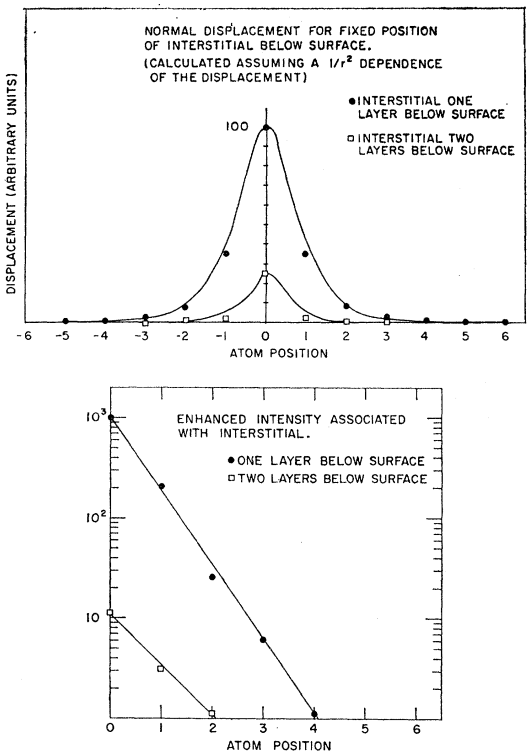

FIG. 10. Schematic representation of enhanced intensity associated with a subsurface interstitial. Normal displacements are calculated for fixed position of interstitial atom, and from this enhanced intensity is assumed proportioned to the cube of the field.

The apparent conditions for observing interstitials are quite stringent, since if it is too far below the surface it is not seen, if it is too close to the surface, field evaporation occurs. The interesting question is, why is the displacement so localized? Two factors must seemingly be considered to rationalize this observation. The first of these is that when an interstitial is observed most clearly, it is observed in a position of relatively low ionization. This can mean that the current-voltage curve value is locally below the best imaging voltage and, since the current in this region depends upon the 30th power of the field,[32] ionization locally depletes the region of helium and more is drawn to this area of ionization.

Secondly, when an interstitial atom is close to the surface, displacements normal to the surface are mainly influential in changing the field, while the tangential displacements are ineffective in the process. This is, of course, exaggerated since on an atomic scale, the planes are atomically flat. Let Δ be the displacement at the surface which is effectively the movement at the atom normal to the surface. Given by

$$\Delta = |\mathbf{r}_0 \cdot \mathbf{n}|/r^2 = |r_0|\,|n|\,x/r^3,$$

where $\mathbf{r}_0$ is a unit vector, $\mathbf{n}$ a unit normal vector, and $\mathbf{r}$ the radial distance that an interstitial is from the surface.

Thus, for a fixed distance below the surface x, atoms at distances r_1 and r_2 undergo normal displacements in the ratio of $(r_1/r_2)^3$. In addition, the enhanced intensity, due to this protuberance, can be estimated by naively using this displacement in conjunction with the field enhancement factor given by Rose. This indicates that an interstitial *does* lead to enhanced intensity over a larger distance than its actual size, as is shown in Fig. 10.

The normal displacements calculated on the basis of $1/r^2$ dependence upon position of the interstitial atom below the surface is used to compute the change in intensity. The displacement is employed as the local protuberance in the field enhancement factor given by Rose[29] and this allows an estimate of the enhanced intensity.

The only reasonable alternative explanation of these results, which we think plausibly explains this result, is that interstitials are removed in stage III in neutron-irradiated platinum. Furthermore, the general density of interstitials precludes general trapping by impurities except in special cases. This conclusion implies that one need not invoke models, such as impurity delayed diffusion of interstitials, to account for the observed activation energy in stage-III recovery. One might plausibly say that some delayed diffusion is occurring, but certainly one should "see" huge interstitial clusters in this case, which we do not observe.

Another implication of the conclusion that a free interstitial moves in stage III is that it is not necessary to assume that some untrapping of vacancies occurs in stage III. For example, even if release of a vacancy from a trap does occur how far will the vacancy move during a reasonable time at 100°C? Cottrell[33] gives a convenient expression which permits us to calculate the number of jumps a diffusing defect will make in time t at temperature T:

$n = Atv_0Z \exp(-E_m/kT)$, where k is Boltzmann's constant, E_m is the activation energy for motion of a single vacancy in platinum ~ 1.5, v_0 is some characteristic vibrational frequency, taken as 10^{13}/sec, A is an entropy term, Z is the coordination number of the lattice $= 12$, and t is chosen at 3600 sec.

If we use these typical values, we obtain $n = 10^{-5}$ jumps. While the above estimate of the number of jumps that a vacancy makes at 100°C in an hour indicates no appreciable motion of the vacancy and *could lead to the assignment of vacancy motion to stage IV*, one other argument which might be considered is the following: If the activation energy for the process occurring in stage IV in platinum corresponds to the motion of single vacancies as well as the release of

[32] M. J. Southon and D. G. Brandon, Phil. Mag. 8, 579 (1963).

[33] A. H. Cottrell, in *Point Defects in Metals and Alloys* (Institute of Metals, London, 1957).

vacancies from impurities, then the sum of this activation energy with the energy of formation of vacancies, as measured by quenching, should not equal the energy of self-diffusion but should be larger

$$E_{IV}+E_f>E_{SD},$$

where E_{IV} is the activation energy observed in stage IV, E_f is the energy of formation of a single vacancy, and E_{SD} is the energy of self diffusion. In the particular case of platinum, this sum is in good agreement with the observed self-diffusion energy. Two arguments seem plausible at this point: Either a large amount of impurity interaction occurs in the self-diffusion measurements, which seems unlikely at the high temperatures involved, or the value given by E_{IV} is not seriously influenced by binding to impurities. It should also be mentioned that in general values of E_f,[34] obtained by quenching studies, agree quite well with values of E_f determined by combined lattice parameter and length change measurements.[35] These arguments, in our opinion, are not successfully answered by the Corbett, Smith, and Walker model of recovery.

B. Depleted Zones and Their Size Distribution

Irradiation of platinum with fast neutrons introduces damage which is directly observed in the field ion microscope (Fig. 4). This is in contrast to observations made by Ruedl *et al.* using transmission electron microscopy techniques, where no observable damage was noted in neutron-irradiated platinum. Presumably, this would include small dislocation loops since Ashby and Brown[36] have shown that such small loops should be observable by transmission electron microscopy. However, in the case of platinum irradiated with alpha particles, Ruedl *et al.*[18] were able to observe defects using transmission electron microscopy.

These results indicate that the defect introduced by fast neutron irradiation is not observable in platinum by transmission electron microscopy. Field-ion microscopy indicates why depleted zones are not observed by electron microscopy. As the measured size distribution shows [Fig. 4(a)] the spread in size goes from 10 to about 40 Å, the dimensions quoted corresponding to maximum sizes of the depleted zones. These zones are not voids but contain between 70 to 80% atoms, as will be shown below. The elastic displacements introduced by such zones decrease quite rapidly with distance from its center—something like $1/r^2$ [37]—whereas the displacements associated with a dislocation only decrease as $\sim 1/r$.[38] Consequently, observation of depleted zones in a transmission electron microscope would depend primarily upon small difference in local density, whereas dislocations are readily observed because of diffraction contrast introduced by the slowly varying displacements associated with dislocations. This qualitative discussion indicates that size measurements of radiation damage, using transmission electron microscopy, might not be capable of recording the presence of small depleted zones.

Closely related to this point is the comparison of the observed size distribution of depleted zones with the energy spectrum of the neutrons which causes the damage in crystals. In the experiments concerned with this point, the specimens were placed in a position in the reactor where it is considered that the spectrum of fast-neutron energies would closely follow a $1/E$ distribution.[39] Secondly, the observed data most closely match an l^{-3} dependence, where l is the maximum measured diameter of a depleted zone. Another point worth mentioning is that the total number of depleted zones measured in this experiment is in the order-of-magnitude agreement with the number expected from standard estimates, knowing the cross sections for this damage as well as the integrated flux. Since this measured number is lower than the theoretical value, a number of explanations such as annealing, direct recombinations, and destruction of zones by focused interstitials, can be invoked. In other words, if the measured numbers were larger than the calculated ones then one could place no confidence in the measurement. A further correlation with mechanical properties of irradiated platinum will be discussed in a subsequent paper.

Some consideration of the observed shapes of the particular depleted zones is also of interest, because of their obvious sensitivity to the method of measurement. As mentioned above and discussed in more detail below, the relative density of atoms in these depleted zones is estimated at around 80%. The observed shapes of the disturbed region were quite isotropic and no systematic differences were noted in the shapes of depleted zones as a function of the sizes. The two main ways in which distortion of the observed depleted zones can be introduced are through the field-evaporation process and the electrostrictive stresses associated with the electric field. During field evaporation in or around a depleted zone, atoms at the surface might be expected to have less than the normal number of neighbors below the surface, and accordingly, evaporate at a lower field than those in more regular surface sites. If the field necessary for imaging is in fact significantly altering the defect structure, the size distribution should not be identified with the energy distribution of the neutrons and thermal annealing should not have a distinct effect upon the larger depleted zones, i.e., there should be no decrease in the upper limit of the size of the depleted

[34] J. E. Bauerle and J. S. Koehler, Phys. Rev. **107**, 1493 (1957).
[35] R. O. Simmons and R. W. Balluffi, Phys. Rev. **117**, 52 (1960).
[36] M. F. Ashby and L. M. Brown, Phil. Mag. **8**, 1083 (1963).
[37] J. D. Eshelby, in *Solid State Physics*, edited by F. Seitz and D. Turnbull (Academic Press Inc., New York, 1956), Vol. 3, pp. 79–106.
[38] A. H. Cottrell, *Dislocations and Plastic Flow in Crystals* (Oxford University Press, New York, 1952).
[39] F. Floyd (private communication).

zones upon annealing. Since a correlation with the energy distribution of the neutrons used as well as some correlation of annealing experiments has been observed we consider this an indication that preferential field evaporation is not introducing serious effects. The stresses introduced by the electrostatic field are presumably hydrostatic in nature and only uniformly expand the structure, which is not expected to seriously disturb the defects present at the temperature of observation.

A general comment can be made regarding the observed annealing in stage I in platinum since it bears on the stability of depleted zones. In the observed recovery in neutron-irradiated platinum, the same fine structure is observed in platinum whether one uses fast neutrons or slow neutrons. The latter predominantly introduce Frenkel defects and one is then justified in assuming that this gives the observed substages of recovery in platinum irradiated with "fast" and "slow" neutrons. This conclusion implies that, if rearrangement of depleted zones occurs in stage I, little, if any, resistivity change is associated with it. This implies that depleted zones are not changed until at least stage IV, since we see no change in the zones until this temperature range.

C. Changes in the Distribution of Vacancy-Type Defects with Annealing

(*i*) *Annealing Temperature 100°C*

In those specimens irradiated at 100°K and annealed at 280°K, and specimens irradiated at 340°K, no observable difference in the distribution of depleted zones was discernible (Fig. 7). This observation can also be interpreted as the removal of interstitial type defects at vacant lattice sites, since annealing at higher temperatures shows that vacancies and small clusters thereof are removed around 350°C. Furthermore, as discussed in Sec. A above, interstitial atoms are removed in this same temperature range.

(*ii*) *Annealing Range 300 to 500°C*

This is the first temperature range where distinctly observable changes in the size distribution of depleted zones occurs (Fig. 8). There are two major changes which are noticeable in the distribution after annealing in this temperature range: The smaller size depleted zones have decreased in number while the larger clusters have also decreased. Concurrently, a new type of defect is observed (Fig. 8) a dislocation loop. A rather straightforward interpretation of this is that vacancies are mobile in this temperature range and that they migrate to larger clusters causing them to collapse to form dislocation loops. The decrease in number of depleted zones on the other end of the size distribution curve is similarly accounted for by vacancies increasing the size of the intermediate size clusters and thereby, shifting the center of gravity of the distribution towards intermediate size clusters. Measurement of the activation energy associated with this process by resistivity measurement[20] as well as changes in the yield stress[40] reveal that the process occurs with an energy of about 1.5 eV.

The collapse of the larger size clusters allows us to give three additional arguments about the annealing stage centered around 350°C. Since the transformation from depleted zones to dislocation loops occurs when the major axis of the depleted zone is in the range of 45 Å and the size of the resultant dislocation loops has been measured, an estimate of the number of vacancies in a depleted zone can be obtained as follows:

$$\text{Number of vacancies in loop} = \pi R_2^2/\pi r_1^2,$$

where R_2 is the radius of a loop, r_1 that of a vacancy.

Number of vacancies in a void the same size as largest depleted zones $= \frac{4}{3}\pi R_2^3/\frac{4}{3}\pi r^3$. The ratio of the two gives the vacancy density in a depleted zone to be 25%.

A second consideration involves the energy of the dislocation loop, $\sim Gb^2R$, which must be equal to or greater than the surface energy of the depleted zone when it collapses. We measure R, use known values of G and b and equate

$$Gb^2R \ln R/r_0 \text{ to } (4n/3)(\pi r^3) \times \text{surface energy } (\gamma)$$

so that

$$(\gamma) \text{ surface energy} = \tfrac{3}{4}(Gb^2R/\pi n r^3)(\ln R/r_0),$$

where n is the number of vacancies in the cluster just prior to collapse and we neglect a term involving the dependence of surface energy upon curvature. The value obtained is $\sim$2200 ergs/cm^2, in agreement with an estimate given by Shewmon of 2000 ergs/cm^2.[41]

A third consideration which arises in connection with this transformation of a depleted zone to a dislocation loop is how the collapse of a void to a planar-type loop takes place without some plastic deformation. While it is true that the energy consideration given above prevails at the time when the transformation occurs and the depleted zone has grown by absorption of vacancies to such a size as to collapse, the collapse itself apparently does not involve any plastic deformation. If this is so, one way of explaining it is by postulating that individual clusters in a depleted zone increase in size and then overlap, the overlap occurring at the edges. The islands of atoms left in this arrangement could then easily rearrange at the periphery. Such a mechanism would not involve deformation nor would it require a change in the internal stress system to nucleate the transformation.

---

[40] J. M. Galligan and M. J. Attardo (unpublished).
[41] P. G. Shewmon (private communication).

(*iii*) *Annealing Range 500 to 600°C*

In this temperature range the remaining depleted zones and the dislocation loops are removed. It is expected that this process would occur with an activation energy roughly corresponding to that for self-diffusion. However, the intermediate size depleted zones must, on the average, emit vacancies rather than absorb them in order to shrink as observed.

Another question which remains is how this process would occur with an activation energy corresponding to self-diffusion. Since in the series process of the depleted zone emitting a vacancy and this vacancy diffusion to, say, a dislocation loop, the energy of motion of a vacancy would be involved, the remainder must be the energy of formation of a vacancy. This latter process could occur simply by the usual accepted ideas of a surface acting as a source for a vacancy: the surface is now the edge of a void within some depleted zone.

V. SUMMARY AND CONCLUSION

In summary the following conclusions can be drawn from this work:

(a) Free single interstitials are removed from neutron irradiated platinum in stage III.

(b) The observed anisotropy of the interstitials has been analyzed and the axis found to be ⟨100⟩.

(c) Depleted zones are a common type of damage site in neutron-irradiated platinum. The observed upper limit on the size of such depleted zones is about 40 Å in diameter.

(d) The presence of depleted zones indicates that a dynamic crowdion is metastable in platinum, at least to the extent necessary to give depleted zones.

(e) The size distribution of depleted zones is consistent with neutron-energy spectrum varying as $1/E$.

(f) Larger depleted zones—above 40 Å in diameter—transform to vacancy dislocation loops with a {110} habit plane, when irradiated specimens are annealed at and above stage IV.

(g) In conjunction with the conditions associated with the transformation from depleted zones to loops, two estimates can be made: (1) The relative density in depleted zones is of the order of 75%; (2) the surface energy of platinum is about 2000 ergs/cm².

(h) Annealing at 280 and 373°K of neutron irradiated platinum, irradiated at 100°K, reveals no drastic change in the depleted zone size distribution and this distribution is consistent with specimens irradiated at 340°K.

(i) On the other hand, annealing of irradiated platinum at 773°K increases the number of depleted zones in the intermediate size range, while small size zones are removed.

(j) Annealing irradiated platinum above 873°K removes all vestiges of damage introduced at lower temperatures.

(k) From changes in the size distribution of depleted zones in stage IV of the irradiated materials, it can be concluded that vacancies are responsible for this change and that vacancies are only mobile in stage IV.

(l) The number of depleted zones increases linearly with integrated flux from 10^{16} through 10^{18} ($E \geq 1.45$ MeV).

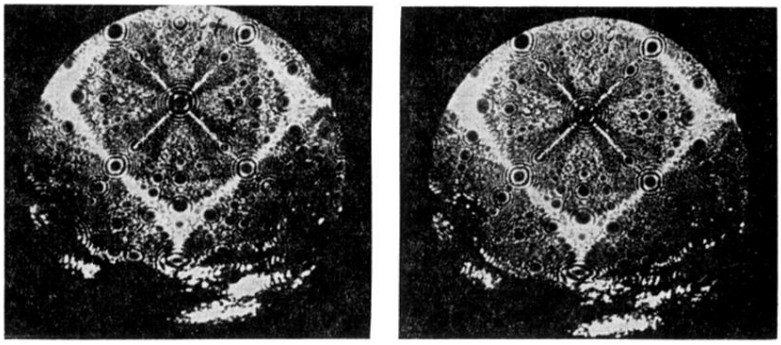

(a) (b)

FIG. 2. Micrograph of platinum specimen bombarded at 4.2°K. Figure 2(a) shows specimen prior to bombardment, while 2(b) shows some interstitial atoms below the surface, as revealed by field evaporation.

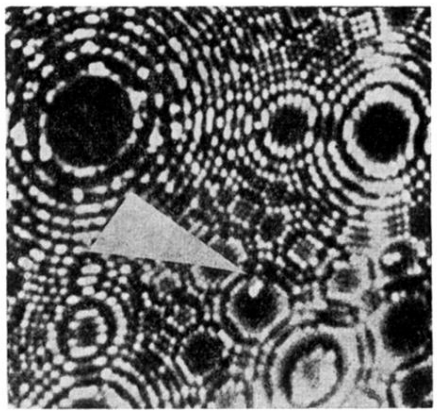

FIG. 3. Bright spots in neutron irradiated platinum, which are present prior to annealing above stage III.

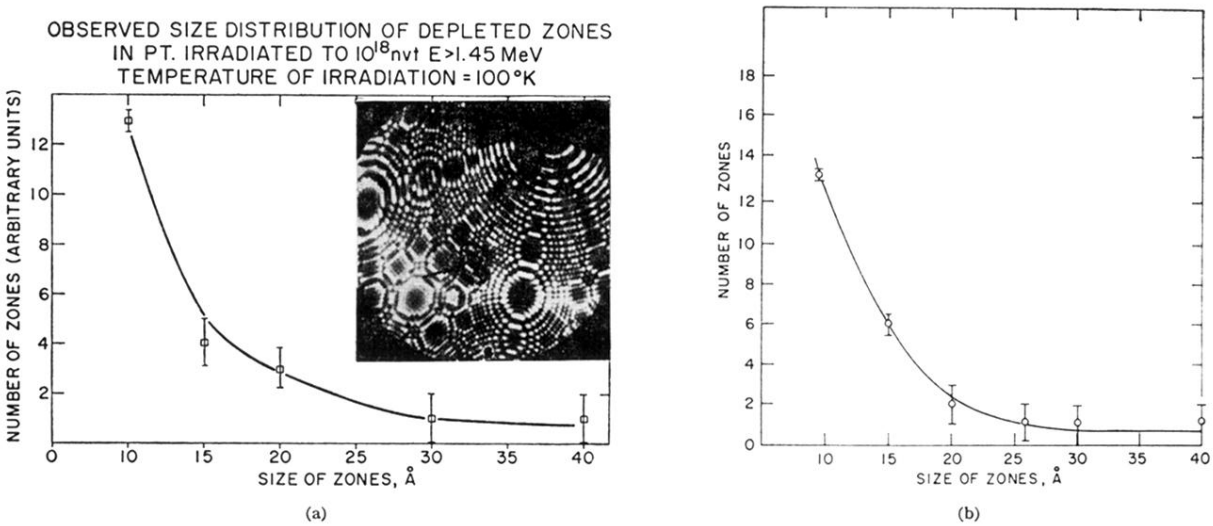

FIG. 4. (a) Size distribution of depleted zones. Photomicrograph of depleted zone in neutron irradiated platinum along with the specimen irradiated at 100°K with fast neutrons ($E>1.45$ MeV) and annealed at 280°K. (b) Size distribution of depleted zones after annealing through stage III.

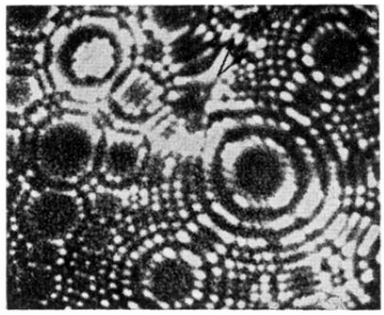

FIG. 5. An example of some defect structures in neutron irradiated platinum after annealing at 373°K.

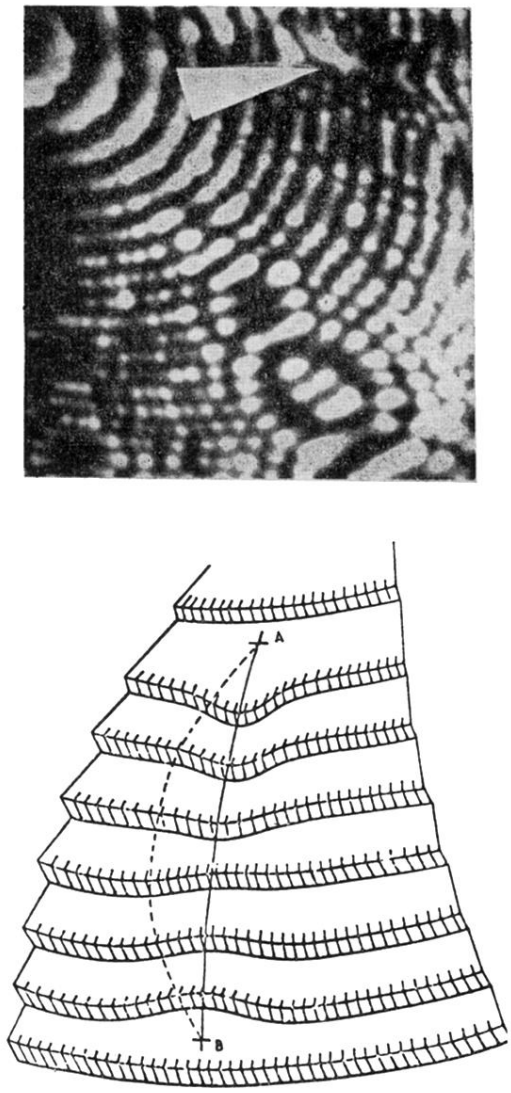

FIG. 8. Vacancy dislocation loop in irradiated platinum after annealing above stage IV (823°K) along with a schematic diagram of contrast effect associated with dislocation loop of approximately 30 Å in size. [After Fortes and Ralph, Phil. Mag. 14, 198 (1966).]